Induced pluripotent stem cell - derived neurons for the study of spinocerebellar ataxia type 3

Hansen, Susanne Kofoed; Stummann, Tina C.; Madsen, Helena Borland; Hasholt, Lis Frydenreich; Tümer, Zeynep; Nielsen, Jørgen Erik; Rasmussen, Mikkel Aabech; Nielsen, Troels Tolstrup; Daechsel, Justus C. A.; Fog, Karina; Hyttel, Poul

Published in:
Stem Cell Research

DOI:
10.1016/j.scr.2016.07.004

Publication date:
2016

Document version
Publisher's PDF, also known as Version of record

Stem Cell Research 17 (2016) 306–317

Contents lists available at ScienceDirect

Stem Cell Research

journal homepage: www.elsevier.com/locate/scr

Induced pluripotent stem cell - derived neurons for the study of spinocerebellar ataxia type 3

Susanne K. Hansen [a,b,*], Tina C. Stummann [b], Helena Borland [b], Lis F. Hasholt [c], Zeynep Tümer [d], Jørgen E. Nielsen [c,e], Mikkel A. Rasmussen [a,1], Troels T. Nielsen [e], Justus C.A. Daechsel [b], Karina Fog [b], Poul Hyttel [a]

[a] Department of Veterinary Clinical and Animal Sciences, University of Copenhagen, Groennegårdsvej 7, 1870 Frb C, Denmark
[b] H. Lundbeck A/S, Ottiliavej 9, Valby 2500, Denmark
[c] Institute of Cellular and Molecular Medicine, University of Copenhagen, Blegdamsvej 3B, 2200 N, Denmark
[d] Applied Human Molecular Genetics, Kennedy Center, Department of Clinical Genetics, Copenhagen University Hospital, Rigshospitalet, Gl. Landevej 7, Glostrup 2600, Denmark
[e] Neurogenetics Clinic & Research Laboratory, Danish Dementia Research Centre, Rigshospitalet, University of Copenhagen, Blegdamsvej 9, 2100 Copenhagen, Denmark

ARTICLE INFO

Article history:
Received 18 March 2016
Received in revised form 9 June 2016
Accepted 18 July 2016
Available online 16 August 2016

ABSTRACT

The neurodegenerative disease spinocerebellar ataxia type 3 (SCA3) is caused by a CAG-repeat expansion in the *ATXN3* gene. In this study, induced pluripotent stem cell (iPSC) lines were established from two SCA3 patients. Dermal fibroblasts were reprogrammed using an integration-free method and the resulting SCA3 iPSCs were differentiated into neurons. These neuronal lines harbored the disease causing mutation, expressed comparable levels of several neuronal markers and responded to the neurotransmitters, glutamate/glycine, GABA and acetylcholine. Additionally, all neuronal cultures formed networks displaying synchronized spontaneous calcium oscillations within 28 days of maturation, and expressed the mature neuronal markers NeuN and Synapsin 1 implying a relatively advanced state of maturity, although not comparable to that of the adult human brain. Interestingly, we were not able to recapitulate the glutamate-induced ataxin-3 aggregation shown in a previously published iPSC-derived SCA3 model. In conclusion, we have generated a panel of SCA3 patient iPSCs and a robust protocol to derive neurons of relatively advanced maturity, which could potentially be valuable for the study of SCA3 disease mechanisms.

1. Introduction

Spinocerebellar ataxia type 3 (SCA3) is a rare autosomal dominantly inherited neurodegenerative disease caused by a CAG-repeat expansion mutation in the *ATXN3* gene, coding for a polyglutamine (polyQ) stretch in the protein ataxin-3. In healthy individuals, the CAG-repeat length spans from 10 to 51, whereas the repeat length in SCA3 patients ranges from 45 to 87, thus 45 to 51 repeats can result in either healthy or disease phenotypes (Matos et al., 2011). Although expanded (exp)-ataxin-3 is expressed throughout the human body (Paulson et al., 1997), only certain brain areas are affected in SCA3. Magnetic resonance imaging and macroscopic investigations of SCA3 brains have revealed severe atrophy of the hindbrain (cerebellum and brain stem) (Rüb et al., 2006; Scherzed et al., 2012). Histological studies have confirmed neuronal loss in these areas and several other brain areas (reviewed by Rüb et al., 2008). This degeneration results in a variety of symptoms of which the most common is progressive ataxia (Matos et al., 2011). Ultimately, SCA3 patients encounter approximately 15 years reduction in life expectancy (Kieling et al., 2007).

Although the CAG-expansion in *ATXN3* is known to cause SCA3, the underlying cellular mechanisms leading to neurodegeneration are not fully elucidated. It has been proposed that the polyQ expansion alters normal ataxin-3 functions in for example endoplasmic reticulum associated degradation (ERAD) and transcriptional regulation (Matos et al., 2011). The polyQ repeat expansion also leads to the formation of SDS-insoluble exp.-ataxin-3 aggregated oligomers and large neuronal intranuclear inclusions (NIIs) (Ellisdon et al., 2006), of which especially the oligomers are thought to be toxic (Pellistri et al., 2013). Aggregates can sequester proteins from diverse cellular processes (Chai et al., 2002; Matos et al., 2011; Mori et al., 2012) and may also disturb the cellular quality control systems, such as the ubiquitin proteasome system and autophagy by overloading (Matos et al., 2011). A prevailing hypothesis is that cleavage of exp.-ataxin-3 is important for its aggregation, as C-terminal polyQ containing fragments of exp.-ataxin-3 seed ataxin-3 aggregation and induce cell death to a higher extend than full length exp.-ataxin-3 (Goti, 2004). Additionally, fragments of ataxin-3 have been detected in affected brain areas of SCA3 patients but not in unaffected areas or in brains of healthy

* Corresponding author at: Department of Veterinary Clinical and Animal Sciences, University of Copenhagen, Groennegårdsvej 7, 1870 Frb C, Denmark.
E-mail address: sus.khansen@gmail.com (S.K. Hansen).
[1] Present address: Bioneer A/S, Kogle Alle 2, 2970 Hoersholm, Denmark.

http://dx.doi.org/10.1016/j.scr.2016.07.004

controls (Goti, 2004). In particular the role of calpain-mediated ataxin-3 cleavage in SCA3 pathogenesis is supported by convincing evidence (Hübener et al., 2013; Koch et al., 2011).

Functional studies investigating molecular mechanisms of neurodegenerative diseases are generally limited by the lack of reliable *in vitro* models of human neurons. Induced pluripotent stem cell (iPSC)-derived neurons are a potential solution to this problem and several disease models have already been generated and published (Reviewed by Corti et al., 2015). The first iPSC lines derived from SCA3 patients were reported by Koch et al. (Koch et al., 2011). In that study, SDS-insoluble exp.-ataxin-3 aggregates could be induced by stimulation with glutamate. This aggregation could be prevented by calpain inhibition, supporting the hypothesis that glutamate induced calcium influx activates calpains, which subsequently mediates the cleavage and aggregation of exp-ataxin-3. In the present study, we aimed at creating iPSCs from SCA3 patient fibroblasts by a non-integrating method, as integration of reprogramming vectors might lead to insertional mutagenesis and has been shown to decrease the differentiation capacity of iPSCs (Sommer et al., 2010). We strived to obtain a model system with increased resemblance to the affected regions of SCA3 brains by applying a differentiation method, which favored the development of hindbrain neurons. Furthermore, we sought to obtain mature neurons to approximate the situation in SCA3 patients where pathology develops in late childhood at earliest (Kieling et al., 2007). Finally, we investigated whether glutamate-induced SDS-insoluble exp-ataxin-3 aggregates similar to those detected by Koch et al. could be observed in our neurons.

2. Materials and methods

2.1. Reprogramming of fibroblasts to iPSCs

The study was approved by the Ethics Committee of the Capital Region of Denmark (H-4-2011-157), and written informed consent was obtained from all patients before enrollment. iPSC lines were created from two SCA3 patients (patient characteristics are summarized in Table S1). SCA3 patient dermal fibroblasts were obtained from forearm skin biopsies and reprogrammed as previously described (Hansen et al., 2016a, 2016b). Briefly, fibroblasts were electroporated with the episomal plasmids pCXLE-hUL (*L-MYC, LIN28*, Adgene #27080), pCXLE-hSK (*SOX2, KLF4,* Adgene #27078) and pCXLE-hOCT4-shp53-F (*OCT4, shP53*, Adgene #27077) (Okita et al., 2011). iPSCs were cultured in mTeSR1 (Stem Cell Technologies, 05850) with 0.1 % penicillin-streptomycin (ThermoFisher Scientific, 15140-122) on hESC-qualified matrigel (BD Biosciences, 354277). Three well-characterized control iPSC lines [K1_shP53 (K1), K2_shP53 (K2) and K3_shP53 (K3), deposited in the European Bank of induced Pluripotent Stem Cells (EBiSC) as BIONi010-A, BIONi010-B and BIONi010-C, respectively] derived from normal human dermal fibroblasts (Lonza, CC-2511) applying the same reprogramming protocol (Rasmussen et al., 2014) were also investigated in this study.

2.2. Neuronal differentiation

Differentiation of iPSCs to neural stem cells (NSCs) was performed using pluripotent stem cell (PSC) neural induction medium (ThermoFisher Scientific, A1647801). iPSCs were treated with neural induction medium (NIM) containing 98% neurobasal medium (ThermoFisher Scientific, 21103-049), 2% PSC neural induction supplement (ThermoFisher Scientific, A1647801) and 0.1% penicillin-streptomycin for 7 days. Day 7, non-neural cells were manually removed and the cells were split with accutase (ThermoFisher Scientific, A1110501) and seeded on 100 μg/ml poly-L-ornithine (PLO) (Sigma-Aldrich, P3655) and 10 μg/ml laminin (LAM) (Sigma-Aldrich, L2020) in neural expansion medium (NEM) supplemented with 10 μM Rock inhibitor (Sigma-Aldrich, Y0503). NEM consisted of 49% neurobasal medium (ThermoFisher Scientific, 21,103–049), 50% Advanced DMEM/F-12 (ThermoFisher Scientific, 12,634), 1% PSC neural induction supplement (ThermoFisher Scientific, A1647801) and 0.1% penicillin-streptomycin. Day 13, the cells were split with accutase and seeded at a density of 1.56×10^5 cells/cm^2 for expansion in NEM with Rock inhibitor. Between day 16–19 NSCs (p2) were frozen in NEM supplemented with 10% DMSO and 10 μM Rock inhibitor (Sigma-Aldrich, Y0503). NSCs were thawed (p3), plated at a density of 1.56×10^5 cells/cm^2 expanded and frozen in larger stocks for experiments (p4). For maturation, NSCs (p6) were seeded at a density of 1.56×10^5 cells/cm^2 in NEM supplemented with 10 μM Rock inhibitor on PLO/LAM (day 0). From day 1–28 of maturation, medium was changed to neuronal maturation medium (NMM) consisting of 50% DMEM/F12 (ThermoFisher Scientific, 31,331) and 50% neurobasal medium, supplemented with 0.5× N2 (ThermoFisher Scientific, 17,502–048), 0.5× B-27 with vitamin A (ThermoFisher Scientific, 17504-044), 1.48 mM glutamax-I (ThermoFisher Scientific, 35,050–061), 0.5× non-essential amino acids (ThermoFisher Scientific, 11140-050), 50 μM 2-mercaptoethanol (ThermoFisher Scientific, 21985-023), 2.5 μg/ml insulin (Sigma-Aldrich, 19,278), 0.1% penicillin-streptomycin, 20 ng/ml brain-derived neurotrophic factor (BDNF) (RnD Systems, 248-BD), 10 ng/ml glial cell derived neurotrophic factor (GDNF) (RnD Systems, 212-GD) and 200 μM ascorbic acid (AA) (Sigma-Aldrich, A5960). 500 μM dibutyryl cyclic adenosine monophosphate (db-cAMP) (Sigma-Aldrich, D0627) was added to the medium from day 1 to day 21–28. Medium was changed every 2 days. Day 7 the cells were split with accutase, seeded at a density of 1.56×10^5 cells/cm^2 on PLO/LAM in NEM with Rock inhibitor and cultured until evaluation in NEM.

2.3. Characterization of iPSCs

The SCA3 iPSC lines were investigated for karyotype, plasmid integration, expression of pluripotency marker mRNA and protein, *in vitro* differentiation and CAG-repeat length as previously described (Hansen et al., 2016a, 2016b).

2.4. Quantitative real time polymerase chain reaction (qRT-PCR)

For characterization of the neuronal differentiation, cells were harvested and reverse transcribed into cDNA with Fast SYBR Green Cells-to-C_T Kit (Ambion, 4402957) according to manufacturer's instructions. RNA from adult whole brain (6516–1) and fetal whole brain week 22–30 (636,118) was purchased from Clontech. Fetal hindbrain week 8,5–9 was kindly provided by Agnete Kirkeby (Lund University). Control RNA was reverse transcribed with TaqMan reverse transcription reagents. qRT-PCR was run with 2× diluted SsoFast EvaGreen Supermix (Bio—Rad, 172–5204). C_T-values were normalized to the geometric mean of the housekeeping genes *Hsp90AB1, GUSB* and *RPL13A* using the $\Delta\Delta C_T$-method. Primers were either conventional primers purchased from Eurofins (Table S2) or Taqman primers purchased from Applied Biosystems (Table S3). The specificity of the conventional primers was validated by standard curves, melting curves and gel electrophoresis.

2.5. Fluorescent immunocytochemistry

For characterization of NSCs and neurons, cells were fixed in 4% paraformaldehyde for 10 min. The cells were blocked in KPBS (0.01 M phosphate buffer with 150 mM NaCl and 3.4 mM KCl) with 0.5% BSA, 0.1% Triton X-100 and 5% normal swine serum (Jackson ImmunoResearch, 014–000-121) for 1 h, incubated with primary antibodies (Table S4) in blocking buffer ON at 4 °C and incubated with secondary antibody and 0.7 μg Hoechst diluted in KPBS for 1 h at RT. The secondary antibodies were used in 1:800 dilution: Alexa 488 donkey-*anti*-mouse (A21202), Alexa 568 donkey-anti-rabbit (A10042), Alexa 488 donkey-anti-goat (A11055), Alexa 594 donkey-anti-rat (A21209) and Alexa 568 goat-anti-mouse (A11031) purchased from ThermoFisher Scientific. The cells were mounted in fluorescent mounting medium (Dako, S3023) and images were captured on a Nikon E1000 microscope and processed with ImagePro Plus v7.0.

Positive and negative cellular controls were used to test the specificity for the majority of the primary antibodies (Table S4). All secondary antibodies were tested for unspecific effects by primary antibody exclusion.

2.6. Western blot

All western blots were performed with standard methods as previously described (Hansen et al., 2016a, 2016b).

2.7. Measurement of intracellular calcium kinetics

Neurons grown in 96-well plates were incubated for 1 h with the fluorescent calcium indicator FLIPR Calcium 5 (Molecular Devices, R8186) diluted in Hanks balanced salt solution (HBSS) (ThermoFisher Scientific, 14175) with 20 mM Hepes (Sigma-Aldrich, H3375) and 1.26 mM $CaCl_2$ (Sigma-Aldrich, C5080). In the experiments investigating neurotransmitter response Calcium 5 was diluted 2× and the cells were incubated and recorded at RT. Response to 300 μM glutamate (Sigma-Aldrich, G100)/10 μM glycine (Sigma-Aldrich, 410,225), 100 μM 5-hydroxy-tryptamine (Sigma-Aldrich, H9523), 25 mM KCl, 100 μM γ-aminobutyric acid (Sigma-Aldrich, A2129), 300 μM acetylcholine (Sigma-Aldrich, A6628) and 100 μM dopamine (Sigma-Aldrich, H60255) was investigated. Three compounds were added in series to each well, one every 10 min. When investigating spontaneous calcium oscillations, cells were incubated at 37 °C in 3× diluted Calcium 5 and HBSS was added after 10 and 20 min, and subsequently 1 μM tetrodotoxin (TTX) (Trocis, 1078) after 30 min. Recordings were performed with an FDSS 7000 Fluorescence Kinetics Plate Reader (Hamamatzu Photonics) (excitation: 480 nm, emission: 540 nm, sampling frequency: 1 Hz).

2.8. Ataxin-3 aggregation and cleavage

2.8.1. Intracellular calcium

The effects of treatments used for cleavage and aggregation experiments on intracellular calcium levels were measured using the protocol described in Section 2.7; however, the incubations were performed at 37 °C with 2× diluted Calcium 5 in BSS and the recordings were performed over a period of 30 min after addition of treatment. Max ratios of quantified traces were calculated as peak responses relative to the baseline before treatment.

2.8.2. Ataxin-3 cleavage

Neurons were treated for 30 min at 37 °C with BSS containing either 100 μM glutamate/10 μM glycine, 100 μM ATP (Sigma-Aldrich, A6419), 1 mM dibucaine (Sigma-Aldrich, D0638) or 0.08–20 μM ionomycin (Sigma-Aldrich, I0634). For calpain inhibition, cells were pre-treated with 200 μM calpeptin for 30 min before adding 100 μM glutamate/10 μM glycine and calpeptin for 30 min. After washing 3× in BSS the cells were harvested in accordance with the Koch protocol (Koch et al., 2011), with the exception that debri and DNA was removed from the lysates by centrifugation at 15,000 g for 10 min to prevent DNA-SDS complexes.

2.8.3. Ataxin-3 aggregation

The ataxin-3 aggregation protocol published by Koch et al. was applied (Koch et al., 2011). One T25 flask 4–10 weeks old neurons was treated 2 × 30 min or 90 min at 37 °C with 100 μM glutamate/10 μM glycine in BSS. A sonication step (5 s 10%, 5 s 50%, repeated 3 times) was introduced after the addition of 2% SDS, to dissolve DNA-SDS complexes.

An ultracentrifugation protocol was also applied to detect smaller SDS-insoluble ataxin-3 aggregates. Neurons were detached with accutase and lysed for 15 min on ice in 250 μl cellytic M cell lysis reagent (Sigma-Aldrich, C2978) with 1 complete protease inhibitor cocktail tablet/40 ml buffer per T25 flask. Samples were sonicated (5 s 10% + 5 s 50%, repeat 3 times) on ice. 2% SDS (IBI scientific, IB07062) was added to the cell lysates before the samples were spun at 20,000 g for 30 min. The supernatants were spun at 186,000 g for 30 min. Before analysis the pellets were thawed and incubated in formic acid (Merck Millipore, 11670) at 37 °C for 16 h to dissolve SDS-insoluble ataxin-3 aggregates and pH was adjusted with 2 M Tris-base before western blot analysis.

2.9. MTT assay

Percentage metabolizing cells was measured with a 3-(4, 5-dimethylthiazolyl-2)-2, 5-diphenyltetrazolium bromide (MTT) assay. Neurons were incubated with 0.5 mg/ml MTT (Sigma-Aldrich, M2128) dissolved in NMM for 1 h at 37 °C. *medium* was removed and crystals were dissolved with 95% isopropanol (ThermoFisher Scientific, 10477070)/5% formic acid. Absorbance was measured at 570 nm and 690 nm, and the percentage of metabolizing cells was calculated as absorbance (570 nm) minus absorbance (690 nm) expressed as percent of BSS treated cells.

3. Results

3.1. SCA3 iPSCs show no integration of episomal plasmids, have normal karyotypes and are pluripotent

Skin fibroblasts from SCA3 patients were isolated and reprogrammed to iPSCs by means of a plasmid-based integration-free methodology (Fig. 1A). Two iPSC lines generated from each of two SCA3 patients (A and B) were investigated in this study (iPSC lines SCA3.A8 (A8), SCA3.A11 (A11), SCA3.B1 (B1) and SCA3.B11 (B11)). The characterizations of A11 and B11 have recently been published (Hansen et al., 2016a, 2016b). The remaining iPSC lines, A8 and *B*1, displayed similar characteristics (Fig. 1). Both iPSC lines had structurally and numerically normal karyotypes (46, XY) (Fig. 1B and S1A) and did not contain DNA originating from episomal plasmids (Fig. 1C). Pluripotency was verified by expression of pluripotency markers at the mRNA (*OCT4, NANOG, SOX2* and *LIN28*) and protein level (OCT4, NANOG, TRA-60-1, TRA-81-1, SSEA-3 and SSEA-4) (Fig. 1D-E, S1B). The gene expression levels were comparable to

Fig. 1. Generation and characterization of SCA3 iPSC lines. A: Timeline of iPSC generation. B: SCA3 iPSCs were karyotyped. At least 10 metaphases were examined (*B*1 shown, A8 in Fig. S1A). C: SCA3 iPSC lines (A8 and *B*1) and parental fibroblasts (H241, H249) were harvested in duplicates and tested for integration of episomal plasmids by qPCR on genomic DNA. C_T–values were normalized to the geometric mean of *Hsp90AB1*, *GUSB* and *RPL13A* and fold change relative to fibroblasts was calculated using the $\Delta\Delta C_T$ –method (mean ± S.D). D: SCA3 fibroblasts, SCA3 iPSCs and the reference iPSCs lines K2 and K3 were harvested in triplicates and reverse transcribed to cDNA for qPCR of pluripotency markers. C_T–values were normalized to the geometric mean of *Hsp90AB1, GUSB* and *RPL13A* and gene expression was calculated relative to fibroblasts (mean ± S.D). E: Fluorescent immunocytochemistry showing expression of pluripotency markers (*B*1 shown, A8 in Fig. S1B). Scalebars: 100 μm. F: Fluorescent immunocytochemistry for α-fetoprotein (AFP) and smooth muscle actin (SMA) in plated *in vitro* differentiated embryoid bodies (*B*1 shown, A8 in Fig. S1C). Scalebars: 100 μm. G: Western blot showing ataxin-3 protein in SCA3 fibroblasts and iPSCs (A8 and *B*1). GAPDH was used to control for equal loading. Two independent experiments were performed and a representative blot is shown. H: Genomic DNA was isolated from duplicate samples of SCA3 fibroblasts (H241 and H249), SCA3 iPSCs (A8, A11, *B*1 and B11), control fibroblasts (NHDF) and control iPSCs (K1, K2 and K3). The CAG-repeat lengths were determined by fragment length analysis.

the levels in the well-characterized iPSC lines K2 and K3. In addition, SCA3 iPSCs could spontaneously differentiate into mesoderm expressing smooth muscle actin (SMA) and endoderm expressing α-fetoprotein (AFP) *in vitro* (Fig. 1F and S1B). Differentiation to ectoderm was demonstrated by directed neuronal differentiation (Section 3.3).

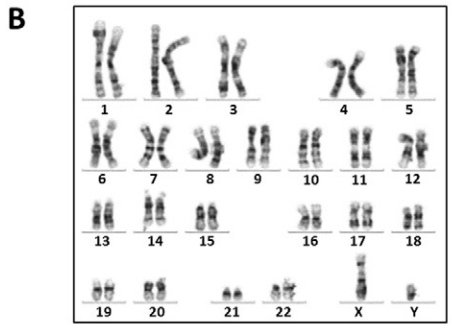

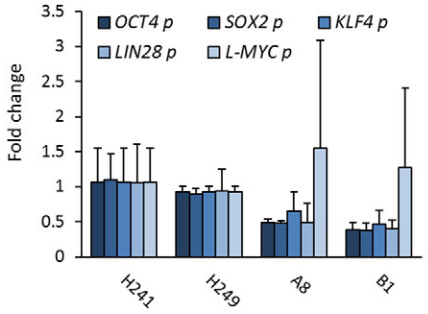

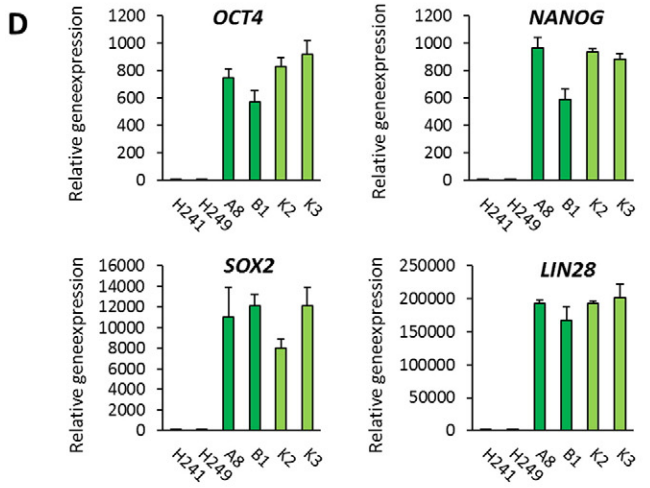

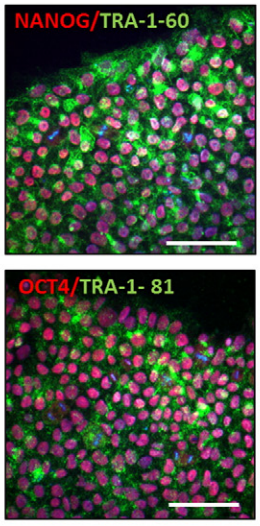

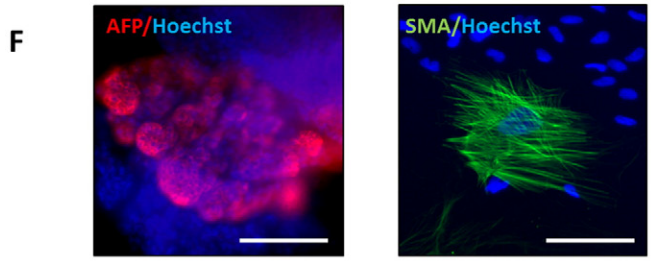

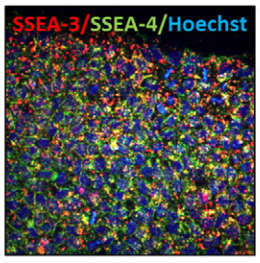

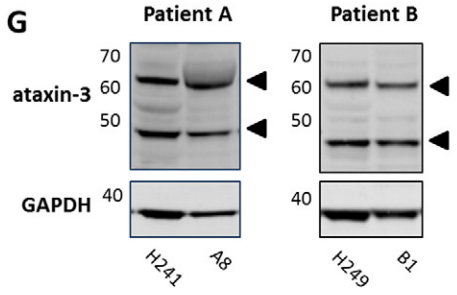

H

	Control A		Patient A		Patient B	
Fibroblasts	NHDF	21/28	H241	23/83	H249	14/74
iPSCs	K1	22/27	A8	23/84	B1	14/73
	K2	22/27	A11	23/83	B11	14/74
	K3	22/27				

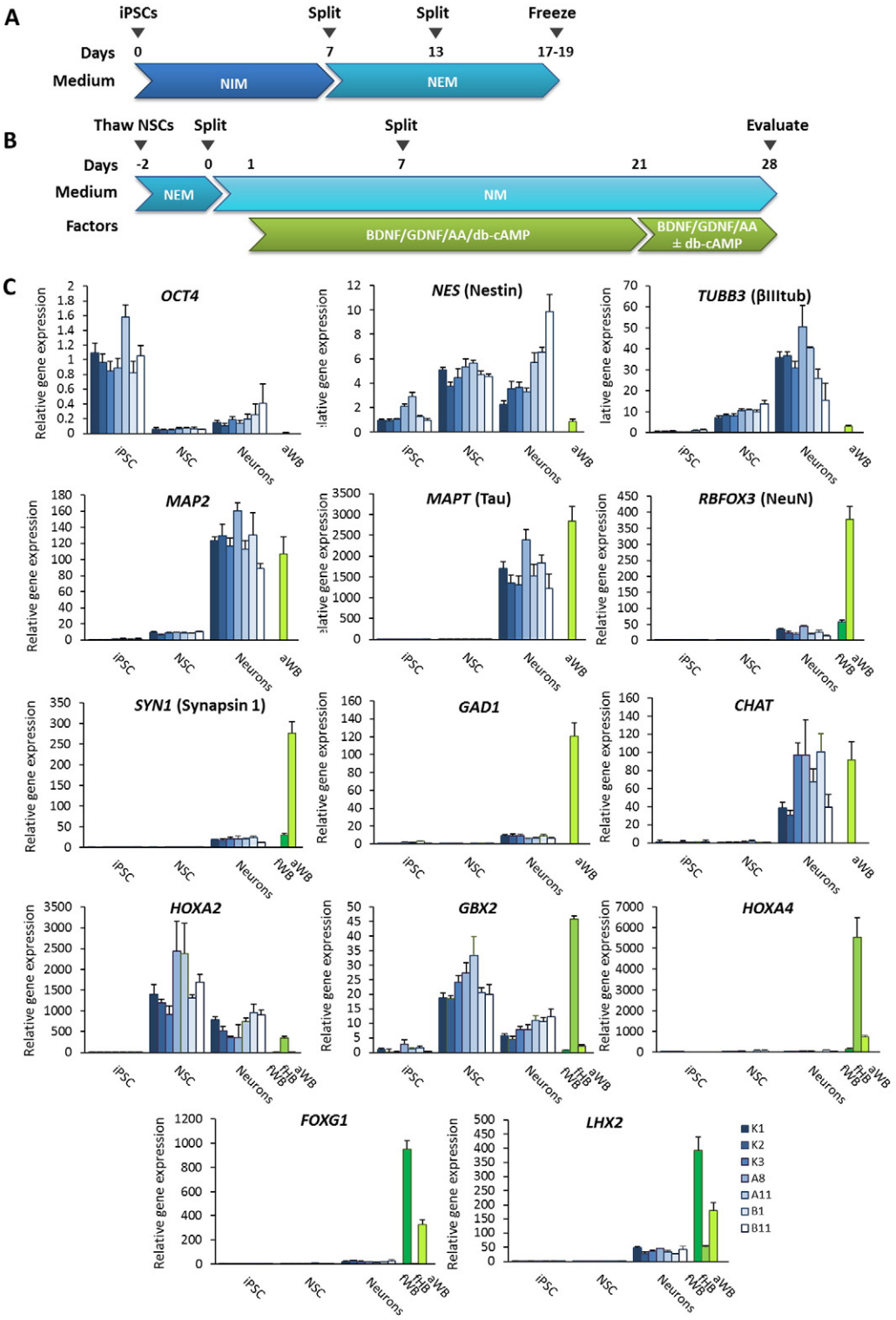

Fig. 2. Gene expression of neuronal markers during neural differentiation. A: Overview of the differentiation of iPSCs to NSCs using PSC Neural induction medium (NIM). Abbreviations: neuronal expansion medium (NEM), Neuronal medium (NM). B: Overview of the neuronal maturation protocol. Abbreviations: Brain-derived neurotrophic factor (BDNF), glial cell line-derived neurotrophic factor (GDNF), ascorbic acid (AA), dibutyryl cyclic adenosine monophosphate (db-cAMP). C: iPSCs, NSCs and neurons were harvested in quadruplicates. cDNA of adult whole brain (aWB) was run as a positive control. Gene expression of pluripotency, NSC and neuronal markers were investigated by qPCR. C_T-values were normalized to the geometric mean of *Hsp90AB1*, *GUSB* and *RPL13A* and gene expression was calculated in relation to iPSCs (mean ± S.D).

3.2. SCA3 iPSCs express ataxin-3 with expanded polyQ repeats

The expression of normal and expanded ataxin-3 protein was detected in SCA3 fibroblasts and iPSCs (Fig. 1G). Fragment length analysis confirmed that the disease alleles were 84 repeats (A8) and 73 repeats (*B*1) (Fig. 1H).

3.3. iPSC-derived neurons express neuronal markers, respond to neurotransmitters and display coordinated spontaneous calcium oscillations

SCA3 and control iPSCs were differentiated to NSCs and subsequently to neurons by the protocol illustrated in Fig. 2A and B. All neuronal lines expressed ataxin-3 protein of expected lengths (Fig. 3C) and it

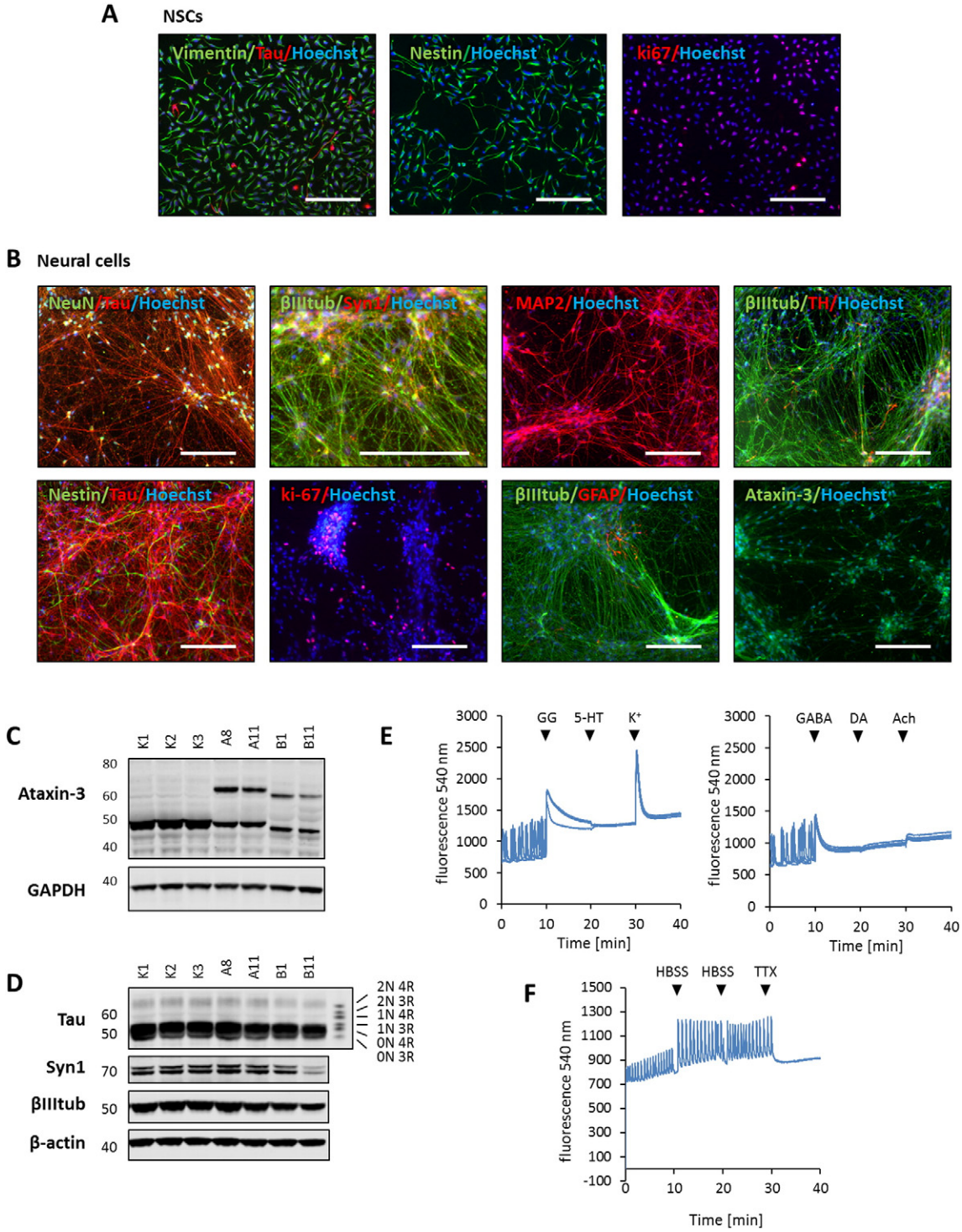

Fig. 3. Protein expression of NSC and neuronal markers, neurotransmitter response and spontaneous calcium oscillations in neuronal cultures. Neuronal differentiation was performed according to Fig. 2A-B (wo db-cAMP d21–28). A: Protein expression of NSC- and neuronal markers in NSCs investigated by fluorescent immunocytochemistry (A11 shown, K1, K2, K3, *B*1, B11 in Fig. S2). Scalebars: 100 μm. B: Protein expression of NSC-, neuronal- and glial markers, and ataxin-3 detected by fluorescent immunocytochemistry in neurons (A11 shown, K1, K2, K3, *B*1, B11 in Fig. S3, S4). Scalebars: 100 μm. C: Western blot showing ataxin-3 expression neurons. GAPDH was used as a loading control. D: Protein expression of neuronal markers determined by western blot with neurons. GAPDH was run as a loading control. A ladder with 6 Tau isoforms (0N3R, 1N3R, 2N3R, 0N4R, 1N4R and 2N4R) is shown. E: Intracellular calcium in response to 300 μM glutamate/10 μM glycine (GG), 100 μM 5-hydroxy-tryptamine (5-HT), 25 mM potassium (K^+), 100 μM γ-aminobutyric acid (GABA), 300 μM acetylcholine (Ach) and 100 μM dopamine (DA) was measured in quadruplicate wells with neurons. All four tracks are shown on the graphs (A11 shown, K1, K2, K3, *B*1, B11 in Fig. S5, S6). F: Synchronized spontaneous calcium oscillations were measured in quadruplicate wells with neuronal cultures. 1 μM TTX was added after 30 min. One representative trace is presented for each neuronal line (a11 shown, K1, K2, K3, *B*1, B11 in Fig. S7).

was located in both soma and neurites of the neurons as expected (Fig. 3B and S4). Gene expression of the pluripotency marker *OCT4* was substantially decreased in NSCs and neurons compared to iPSCs (Fig. 2C) and OCT4 protein could not be detected in the neuronal cultures (data not shown). NSCs and neurons showed similar mRNA upregulation of the NSC marker *NES* (Nestin) (Fig. 2C). Most NSCs expressed Nestin and Vimentin protein (Fig. 3A and S2), while only few Nestin positive cells were present in the neuronal cultures (Fig. 3B and S4). The

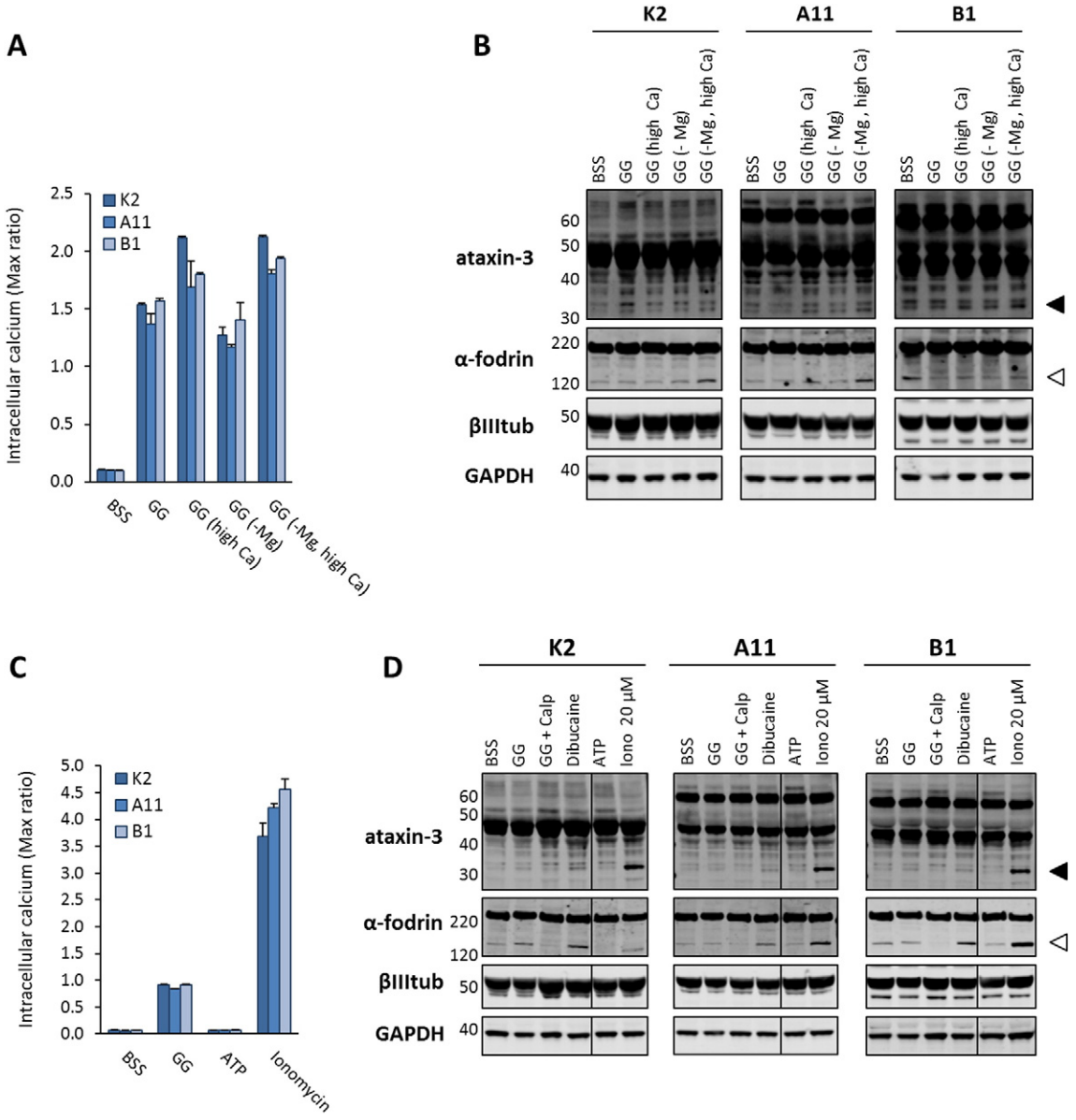

Fig. 4. Attempt to detect SDS-insoluble ataxin-3 aggregates in iPSCs derived neurons. Neural differentiation was performed according to Fig. 2A-B (with db-cAMP d21–28). A: The intracellular calcium levels in response to glutamate (6.25–200 μM) combined with 10 μM glycine were investigated in quadruplicate wells (K2). A trace with 100 μM glutamate and 10 μM glycine (GG) is shown as an example. B: Overview of Koch's protocol for detection of SDS-insoluble ataxin-3 aggregates. C-E: Investigation of SDS-insoluble ataxin-3 aggregates using Koch's protocol. Neuronal cultures were derived from K2, A11 and *B*1 according to Fig. 2A-B, but were additionally cultured in maturation medium with all factors for 10 weeks. C: Verification of intracellular calcium response to GG in triplicate wells. D: Western blots of input samples. Cells were treated for 2 × 30 min with GG and left to recover for 24 h before Koch's protocol for detection of SDS-insoluble aggregates was performed. GAPDH was used as loading control. E: Western blot of SDS-insoluble fractions. F: Overview of the ultracentrifugation protocol for detection of SDS-insoluble ataxin-3 aggregates. G-I: Investigation of SDS-insoluble ataxin-3 aggregates using the ultracentrifugation protocol. Neuronal cultures were derived from K2 and A8. G: Confirmation of intracellular calcium response to GG performed in triplicates. H: Western blot of input samples. Neuronal cultures were treated 2 × 30 min with GG and left to recover for 24 h. GAPDH was run as a loading control. I: Western blot of SDS-insoluble fractions.

proliferation marker Ki-67 was expressed in a higher proportion of cells in NSC cultures compared to neuronal cultures (Fig. 3A, B, S2 and S4). The pan-neuronal markers *TUBB3* (βIIItub), *MAP2* (MAP2), *MAPT* (Tau), *RBFOX3* (NeuN) and *SYN1* (Synapsin 1) were expressed at both mRNA and protein levels in the neuronal cultures (Fig. 2C, 3B, D, S3, and S4). The gene expression levels were higher than, or comparable to, those of adult whole brain, except for the postmitotic marker *RBFOX3* (NeuN) and the presynaptic marker *SYN1* (Synapsin 1) which were both expressed at levels comparable to that of fetal whole brain. In accordance, only a fraction of the cells expressed NeuN and Synapsin 1 protein (Figs. 3B, 4D and S3). Furthermore, only two low bands of Tau protein were present in the neurons (Fig. 3D). The lower band being the embryonal isoform 0N3R Tau, and the upper band most likely being phosphorylated Tau species, based on our previous experiments (data not shown). None of the additional five isoforms expressed in adult human brain were present (Goedert and Jakes, 1990). The hindbrain genes, *HOXA2* and *GBX2* (Kirkeby et al., 2012) were upregulated in NSCs and neuronal cultures at a level comparable to fetal hindbrain. In contrast, the marker of caudal hindbrain *HOXA4* (Philippidou and Dasen, 2013) was not expressed (data not shown). The gene expression of *FOXG1* and *LHX2* primarily expressed in the forebrain (Kirkeby et al., 2012), were comparable to fetal hindbrain and lower than fetal and adult whole brain levels (Fig. 2C). Analysis of gene expression levels of neuronal subtype markers revealed that the gene expression of *CHAT* (cholinergic neurons) was comparable to that of adult whole brain (Fig. 2C), and that *GAD1* (GAD67, GABAergic neurons) was slightly up-regulated in neurons compared to iPSCs; however, not to the level observed in adult whole brain (Fig. 2C). GAD65/67 protein was not

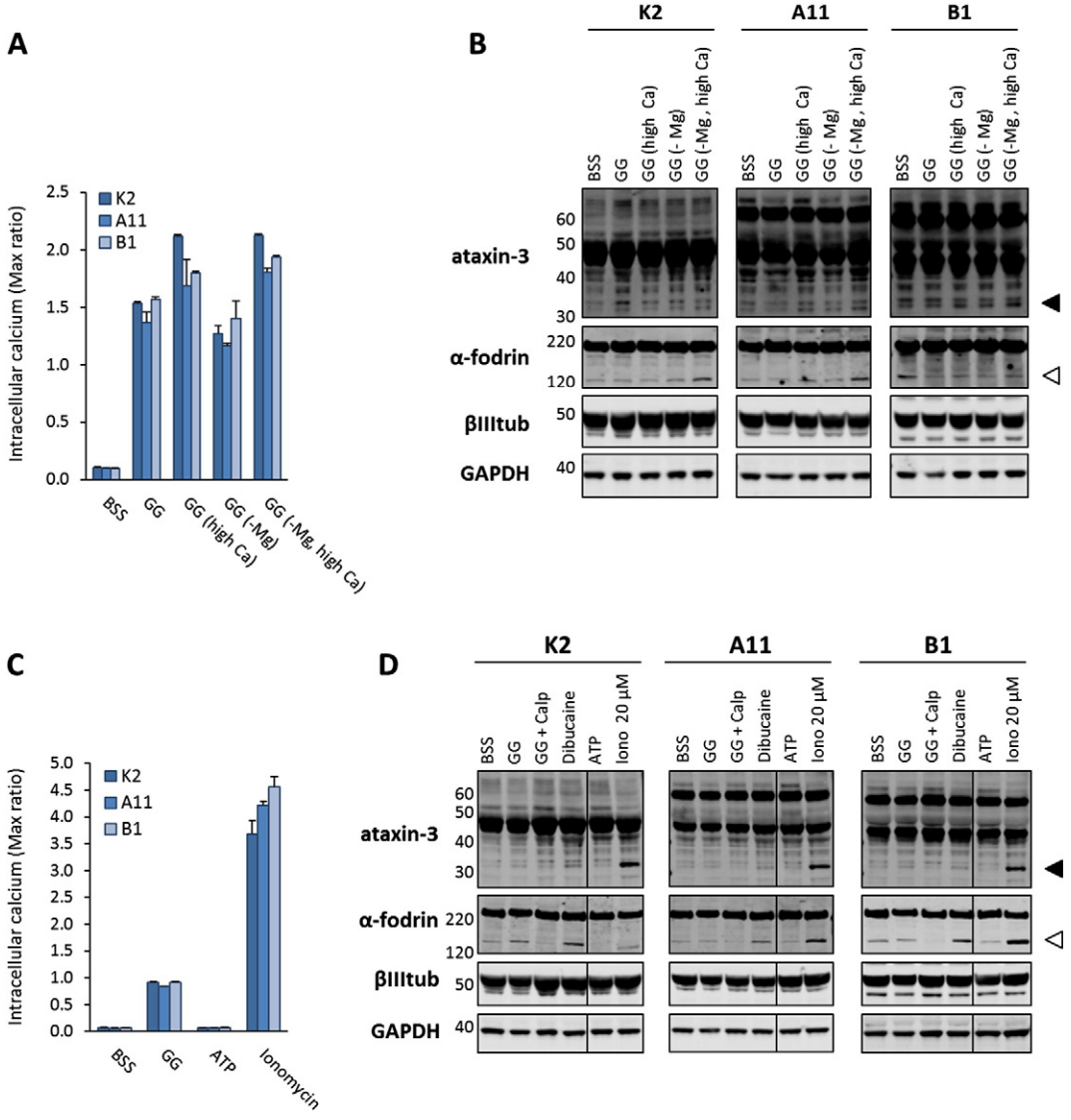

Fig. 5. Induction of ataxin-3 cleavage. Neural differentiation was performed according to Fig. 2A-B (with db-cAMP d21–28). A-B: Effect of extracellular calcium (*Ca*) and magnesium (Mg) concentration on ataxin-3 cleavage was tested in neurons derived from K2, A11 and *B*1. A: Intracellular calcium response to 100 μM glutamate/10 μM glycine (GG) in BSS buffer supplemented with normal (1.8 mM) or high (3.7 mM) $CaCl_2$ combined with either normal (0.8 mM) or no $MgCl_2$ was investigated in duplicate wells. B: Neuronal cultures were treated with GG for 30 min and directly harvested for western blot. Ataxin-3 fragments are marked with black arrows while α-fodrin fragments are marked with open arrowheads. GAPDH was used as a loading control and βIIItub was used to compare the degree of neural differentiation. The extra bands detected at approximately 50 kDa and 60 kDa on the βIIItub blot are weak traces of ataxin-3. C–D: Effect of different treatments on ataxin-3 cleavage in neurons derived from K2, A11 and *B*1. C: Intracellular calcium response to GG, 100 μM ATP and 20 μM ionomycin was tested in duplicate wells. D: Neuronal cultures were treated with GG, 1 mM dibucaine, 100 μM ATP or 20 μM Ionomycin for 30 min and harvested directly. When treated with 200 μM calpeptin, cells were pretreated for 30 min with calpeptin before treatment with GG + calpeptin for 30 min. Ataxin-3 fragments are marked with black arrowheads and α-fodrin fragments are marked with white arrowheads. GAPDH was used as a loading control and βIIItub was used to detect the degree of neural differentiation. The extra bands detected at approximately 50 kDa and 60 kDa on the βIIItub blot are weak traces of ataxin-3. Where blots are divided by black vertical lines, irrelevant samples were removed.

detected (data not shown). A minor fraction of the cells in the neuronal cultures expressed TH (dopaminergic/adrenergic marker) (Fig. 3B and S3). *SLC17A7* (vGLUT1, glutamatergic neurons) was neither detected at the mRNA nor the protein level (data not shown). Furthermore, mRNA of the serotonergic marker *TPH2* was not expressed (data not shown). The majority of the neuronal cultures contained few cells staining positive for the astrocyte marker GFAP (Fig. 3B and S4).

Image based assessment of changes in intracellular calcium levels was used to evaluate the functionality of the neurons. The neurotransmitters, GABA and glycine/glutamate, and membrane depolarization with potassium resulted in a large rise in intracellular calcium levels in all neuronal cultures (Fig. 3E, S5 and S6), while acetylcholine caused a minor and serotonin and dopamine no response. Detection of spontaneous calcium oscillations indicated that spontaneous firing was synchronized between the majorities of the neurons in the 96-wells. The oscillations could be abrogated by the voltage-gated sodium channel blocker TTX (Fig. 3F and S7).

3.4. Glutamate treatments of iPSC derived neurons did not induce SDS-insoluble ataxin-3 aggregates

Exposing SCA3 iPSC-derived neurons to 100 μM glutamate has been reported to induce SDS-insoluble ataxin-3 aggregates (Koch et al., 2011). 100 μM glutamate was also used in the present study as this concentration resulted in maximal increase in intracellular calcium (Fig. 4A). Both the protocol published by Koch et al. (Fig. 4B) and a protocol based on ultracentrifugation (Fig. 4F) were applied to investigate if a patient-specific ataxin-3 aggregation phenotype could be identified. Increase of intracellular calcium in response to the applied treatments was measured in all batches of neurons used for

aggregation and ataxin-3 cleavage experiments. Neither 4 or 10 weeks old neurons investigated with the Koch protocol (Fig. 4C-E and 6B-D) nor 4 weeks old neurons investigated with the ultracentrifugation protocol (Fig. 5G-I) resulted in detectable SDS-insoluble aggregates after treatment with 100 μM glutamate/10 μM glycine for 2 × 30 min followed by 24 h recovery. Increasing the glutamate and glycine stimulation period to 90 min did not induce SDS-insoluble aggregates detectable by Koch's protocol in 4 weeks old neurons (Fig. 6B-D). db-cAMP has been reported to induce proteasome activity (Myeku et al., 2012) and could thereby potentially increase the degradation of exp.-ataxin-3 species. However, withdrawal of db-cAMP for the last week of the differentiation also did not induce SDS-insoluble ataxin-3 aggregates detectable by Koch's protocol in 4 weeks old neurons (Fig. 6B-D).

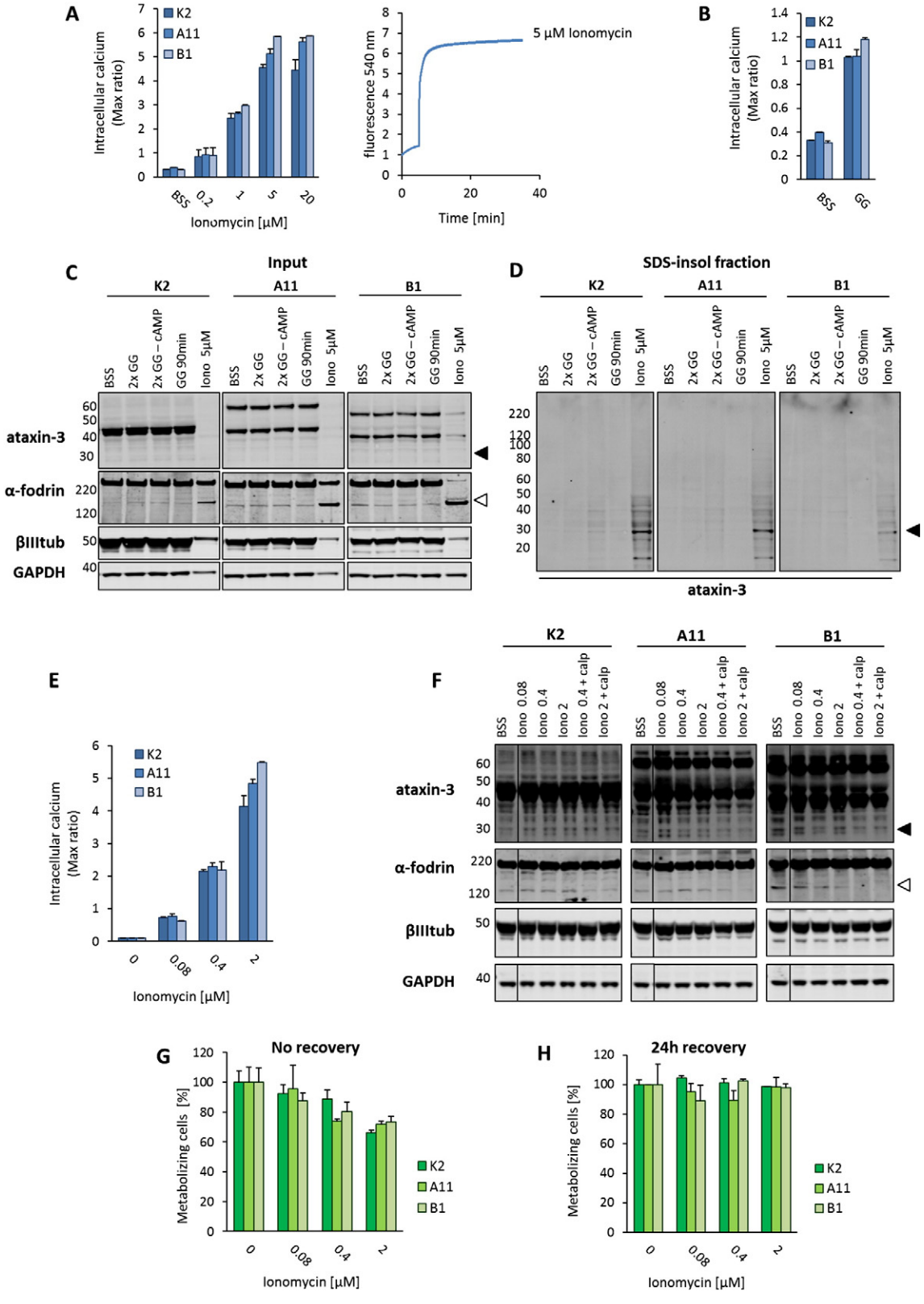

3.5. Ionomycin induced ataxin-3 cleavage in iPSC derived neurons

It has been hypothesized that the glutamate induced intracellular calcium increase activates calpain-mediated ataxin-3 cleavage and thus induces the formation of SDS-insoluble ataxin-3 aggregates (Koch et al., 2011). We decided to test the capability of multiple treatments to induce ataxin-3 cleavage *via* calcium activated calpain and hence identify conditions that potentially induce ataxin-3 aggregation. The calpain substrate α-fodrin was used as an indicator of calpain activity. Calpain seemed to be active to a low extend in the neurons, as the basal level of ataxin-3 and α-fodrin fragments could be partially decreased by the calpain inhibitor calpeptin. However, ataxin-3 and α-fodrin cleavage could only be slightly induced by the calpain activator dibucaine (Zhang et al., 2011) (Fig. 5D).

We optimized the glutamate stimulation conditions to maximize the resulting increase in intracellular calcium (Fig. 5A). Doubling the extracellular calcium concentration resulted in an increase of intracellular calcium in response to glutamate treatment (Fig. 5A), whereas no effect was detected upon magnesium withdrawal. No systematic effects of calcium and magnesium concentrations were observed on the cleavage of ataxin-3 or α-fodrin (Fig. 5B). Furthermore, the effect of the P2Y purinoreceptor agonist ATP and the calcium ionophore ionomycin were tested. ATP had no effect, but ionomycin (20 μM) gave rise to a massive increase in intracellular calcium levels (Fig. 5C) and a marked increase in both ataxin-3 and α-fodrin cleavage (Fig. 5D).

3.6. Ionomycin could not induce ataxin-3 aggregation selectively in SCA3 iPSC derived neurons

Concentration-response experiments with ionomycin established that 5 μM ionomycin was the lowest concentration giving a maximal response in intracellular calcium level (Fig. 6A). The ability of 5 μM ionomycin to induce SDS-insoluble ataxin-3 aggregates was tested with the Koch protocol on 4 weeks old neurons. Aggregates were detected in both control and SCA3 neuronal cultures (Fig. 6D) and therefore were most likely not facilitated by exp.-ataxin-3. During harvest for the aggregation experiment, it was noticed that the cells treated with ionomycin detached more readily compared with other conditions. Together with massive fragmentation of α-fodrin and low levels of ataxin-3 and βIIItub (Fig. 6C), this indicated that 5 μM ionomycin was toxic to the cells in the stimulation paradigm applied (2 × 30 min stimuli, 24 h recovery). It was investigated if the concentration of ionomycin could be decreased (0.08, 0.4, 2.0 μM) in order to avoid toxicity. 2 μM ionomycin appeared toxic when tested just after treatment (Fig. 6G); however, this effect was transient and disappeared after 24 h recovery (Fig. 6H). Furthermore, lower ionomycin concentrations (0.08, 0.4 and 2.0 μM) were unable to induce ataxin-3 or α-fodrin cleavage (Fig. 6F). Taken together, we could not identify an ionomycin concentration inducing ataxin-3 cleavage without showing general cytotoxicity.

4. Discussion

In general, studies of human neurodegenerative disease mechanisms are limited by the lack of human neuronal *in vitro* models. In this study, we report iPSC lines that can form the basis for developing a new improved model system for studying SCA3 disease mechanisms. iPSCs generated from two SCA3 patients (four lines) and one healthy individual (three lines) by reprogramming of dermal fibroblasts with an integration-free method were differentiated into neurons. As the hindbrain is particularly affected by neurodegeneration in SCA3, we applied a neuronal differentiation protocol, which has been reported to give rise to NSCs expressing hindbrain genes such as *HOXA2* and *HOXB2* (Yan et al., 2013). The applied neuronal differentiation method generated large amounts of NSCs from a single neural induction (1 × 6-well of iPSCs can generate 400 vials of 4 million p4 NSCs) which could be easily obtained and frozen. Differentiations from these NSCs have proven to be highly reproducible in our laboratory. Expression of the hindbrain genes *HOXA2* and *GBX2* were increased in all derived NSCs and neurons to levels comparable to fetal hindbrain. In addition, the forebrain markers *FOXG1* and *LHX2* were also expressed at the level of fetal hindbrain. Together, these data indicate that the applied differentiation paradigm resulted in neurons with caudal identity. It has to be kept in mind that the regional markers are transiently expressed during embryo development and that further analysis is need to confirm protein expression and determine the percentage of neurons with hindbrain identity. Investigation of the neuronal subtype indicated cholinergic identity based on mRNA expression when comparing to adult whole brain. Furthermore low expression of GABAergic and dopaminergic markers were also observed. Overall, these results suggest the presence of cholinergic neurons of hindbrain origin. Neuronal cultures from all iPSC lines expressed a range of pan-neuronal markers (*TUBB3* (βIIItub), *MAP2* (MAP2), *MAPT* (Tau), *RBFOX3* (NeuN)) and *SYN1* (Synapsin 1) with only minor differences in mRNA expression levels between the neuronal cultures. The neurons seemed to have reached a certain state of maturity as the postmitotic marker NeuN and the presynaptic marker Synapsin 1 were expressed in subsets of neurons. The gene expression levels of *RBFOX3* (NeuN) and *SYN1* (Synapsin 1) in iPSC-derived neurons were at the level of fetal whole brain but lower than in adult whole brain indicating that some or all of the cells were not fully mature. In line with these observations, only the embryonic isoform of Tau 0N3R (Goedert and Jakes, 1990) was expressed. So far, only one study has detected all adult Tau isoforms in iPSC-derived neurons. Noticeably, they did not arise until day 365 of cell culture (Sposito et al., 2015).

All iPSC-derived neurons demonstrated expression of functional neurotransmitter receptors, responding to glutamate/glycine, GABA and to a lower extend to acetylcholine. Interestingly, the neuronal cultures also developed synchronized spontaneous calcium oscillations, which were likely to reflect action potential firing (Robinson et al., 1993). This was confirmed as the inhibitor of voltage-gated sodium channels, TTX, blocked the synchronization of the oscillations.

In vivo, spontaneous calcium oscillations occur in individual neural precursors and immature neurons in early development where they regulate several processes (Blankenship and Feller, 2009). Both during late embryonic and early postnatal development, neurons from many different areas of the CNS have been shown to form synchronized oscillatory networks consisting of bursts of action potentials separated by periods without firing. Such networks are believed to be mediated by gap junctions during embryonic development, while chemical synaptic transmission tends to mediate the majority of the network activity later

Fig. 6. Effect of ionomycin on ataxin-3 cleavage and aggregation. Neural differentiation of K2, A11 and *B*1 was performed according to Fig. 2A-B. A–D: Investigation of SDS-insoluble ataxin-3 aggregates using the Koch protocol. A: Intracellular calcium levels in response to 0.2–20 μM ionomycin were investigated in quadruplicate wells. A trace with 5 μM ionomycin is shown as an example. B: Intracellular calcium response to 100 μM glutamate/10 μM glycine (GG) was measured in triplicates. C: Input samples. Neuronal cultures were treated for 2 × 30 min or 90 min with GG or 5 μM ionomycin and left to recover for 24 h before testing aggregation. Ataxin-3 fragments are marked with black arrowheads and α-fodrin fragments are marked with open arrowheads. GAPDH was used as a loading control and βIIItub was used to monitor the degree of neural differentiation. The extra signals detected at approximately 50 kDa and 60 kDa on the βIIItub blot are remnants of ataxin-3. D: SDS-insoluble fractions. Ataxin-3 fragments are marked with black arrowheads. *E*-H: Adjustment of the ionomycin dosis to avoid toxicity. E: Intracellular calcium levels in response to 0.04–2 μM ionomycin was tested in duplicate wells. F: Neuronal cultures were treated with 0.04–2 μM ionomycin for 30 min and harvested for western blot. Ataxin-3 fragments are marked with black arrowheads and α-fodrin fragments are marked with open arrowheads. GADPH was used as a loading control and βIIItub was used to indicate the degree of neural differentiation. The extra signals detected at approximately 50 kDa and 60 kDa on the βIIItub blot are remnants of ataxin-3. Where blots are divided by black vertical lines, irrelevant samples were removed. G-H: Fraction of metabolizing cells. Duplicate wells were treated with ionomycin for 30 min and MTT assay was performed G: without recovery or H: with 24 h recovery.

in development and in mature neurons (Blankenship and Feller, 2009; Sutor and Hagerty, 2005). The occurrence of spontaneous synchronized calcium oscillations as well as the expression of the presynaptic protein Synapsin 1 in our neuronal cultures therefore implies a certain level of neuronal maturity. The mediation by chemical synapses could be confirmed by applying inhibitors or knock down of neurotransmitter receptors or gab junctions (Blankenship and Feller, 2009). *In vitro*, synchronized network activity mediated by chemical synapses has been observed in primary (Dravid and Murray, 2004) and ESC derived neurons (Heikkilä et al., 2009). Only recently, such network activity was reported in one study of iPSC derived neurons. However, these neurons had to be cultured for 70–140 days and form 3D structures before regular spontaneous oscillations dependent on chemical synaptic activity were observed (Kirwan et al., 2015). In our neuronal cultures, synchronized spontaneous activity occurred robustly in all cell lines already after 28 days of maturation, which indicated that they have reached a relatively advanced state of maturity compared to the majority of other iPSC derived neurons.

A key element of SCA3 is the presence of SDS-insoluble ataxin-3 aggregates. Here we strived to induce aggregate formation with glutamate stimulation as described previously (Koch et al., 2011), yet, without success. As we were unable to obtain a positive control such as transgenic mouse brain with ataxin-3 aggregates, it was not possible to evaluate the protocols for detection of ataxin-3 aggregates. In addition, several biological traits of the investigated neurons could have inhibited the formation and accumulation of aggregates. Firstly, the neuronal differentiation protocol applied by Koch et al. was significantly different than ours, and likely to have generated a different neuronal population. In support of this, their neurons expressed the GABAergic marker GABA, whereas our cells only expressed GABAergic marker mRNA but not protein. Secondly, it is possible that our neurons are better at clearing cleaved and aggregated ataxin-3. For example, db-cAMP, has been shown to increase proteasomal activity (Myeku et al., 2012) and is used in a 800× lower concentration in the maturation protocol applied by Koch et al. compared to our protocol. However, withdrawal of db-cAMP for the last week of maturation did not induce SDS-insoluble aggregation in our experiments. Finally, our neurons might express less calpain or the calpain-activity might be decreased, reducing the cleavage of exp.-ataxin-3 and, thus, the formation of aggregates. For example, the spontaneous calcium oscillations caused by action potential firing in the neurons could induce prolonged calpain activation, which is known to upregulate the expression of the endogenous calpain inhibitor calpastatin (Averna et al., 2003). Supporting this theory, we were unable to induce high levels of calpain mediated cleavage of ataxin-3 and the calpain substrate α-fodrin using several ways to increase intracellular calcium levels in order to activate calpain, including increased glutamate response, treatment with a calpain activator (dibucaine) and a purinoreceptor agonist (ATP). The ionophore ionomycin, however, increased ataxin-3 and α-fodrin cleavage, but it was not possible to find an ionomycin concentration, which induced ataxin-3 cleavage without being toxic to the neurons. In further experiments, it will be relevant to explore other methods, such as induction of oxidative stress, proteasomal inhibition or inhibition of autophagy to either induce aggregation or cause accumulation of aggregates by inhibiting their degradation.

Although aggregation is a key feature of SCA3, neuronal intra-nuclear inclusions have also been detected in unaffected parts of SCA3 brain (Yamada et al., 2004), indicating that aggregation alone does not cause neurodegeneration. Indeed, no toxicity was induced by the SDS-insoluble aggregates observed in the study by Koch et al. Furthermore, both neurodegeneration and behavioral phenotypes have been observed in a SCA3 mouse model, which did not have neuronal intra-nuclear inclusions or SDS-insoluble aggregates (Silva-Fernandes et al., 2010), indicating that the presence of aggregates is not needed to cause a SCA3 phenotype. The iPSC derived neurons generated in this study, might therefore serve to investigate disease mechanisms not necessarily related to ataxin-3 aggregation, for example alterations in WT ataxin-3 functions caused by the expanded polyQ repeat.

5. Conclusion

We have successfully generated SCA3 patient-derived iPSCs by an integration-free method. Four SCA3 iPSC lines and three control iPSC lines were differentiated into neurons which showed similar expression of pan-neuronal markers and responded to several neurotransmitters. Furthermore, after only 28 days of maturation the expression of the postmitotic marker NeuN and the pre-synaptic marker Synapsin 1 together with synchronized spontaneous calcium oscillations implied a relatively advanced neuronal maturity in comparison with existing iPSC-derived neurons. Although SDS-insoluble aggregates could not be induced in these neurons we believe that the generated neurons could potentially be it a valuable tool for modeling SCA3.

Acknowledgments

We would like to acknowledge Dr. Keisuke Okita and Prof. Shinya Yamanaka for providing the episomal plasmids. Additionally, we thank Charlotte Vajhøj and Tina Christoffersen for skillful technical assistance. We thank SHARE's Cross Faculty PhD Initiative (University of Copenhagen), The Danish National Advanced Technology Foundation (project number 047-2011-1; patient-specific stem cell-derived models for Alzheimer's disease), the European Union Seventh Framework Program (PIAP-GA-2012-324451-STEMMAD) and Innovation Fund Denmark, BrainStem for financial support.

Appendix A. Supplementary data

Supplementary data to this article can be found online at http://dx.doi.org/10.1016/j.scr.2016.07.004.

References

Averna, M., De Tullio, R., Capini, P., Salamino, F., Pontremoli, S., Melloni, E., 2003. Changes in calpastatin localization and expression during calpain activation: a new mechanism for the regulation of intracellular Ca(2+)-dependent proteolysis. Cell. Mol. Life Sci. 60, 2669–2678. http://dx.doi.org/10.1007/s00018-003-3288-0.

Blankenship, A.G., Feller, M.B., 2009. Mechanisms underlying spontaneous patterned activity in developing neural circuits. Nat. Rev. Neurosci. 11, 18–29. http://dx.doi.org/10.1038/nrn2759.

Chai, Y., Shao, J., Miller, V.M., Williams, A., Paulson, H.L., 2002. Live-cell imaging reveals divergent intracellular dynamics of polyglutamine disease proteins and supports a sequestration model of pathogenesis. Proc. Natl. Acad. Sci. U. S. A. 99, 9310–9315. http://dx.doi.org/10.1073/pnas.152101299.

Corti, S., Faravelli, I., Cardano, M., Conti, L., 2015. Human pluripotent stem cells as tools for neurodegenerative and neurodevelopmental disease modeling and drug discovery. Expert Opin. Drug Discovery 10, 615–629. http://dx.doi.org/10.1517/17460441.2015.1037737.

Dravid, S.M., Murray, T.F., 2004. Spontaneous synchronized calcium oscillations in neocortical neurons in the presence of physiological [Mg2+]: involvement of AMPA/kainate and metabotropic glutamate receptors. Brain Res. 1006, 8–17. http://dx.doi.org/10.1016/j.brainres.2004.01.059.

Ellisdon, A.M., Thomas, B., Bottomley, S.P., 2006. The two-stage pathway of ataxin-3 fibrillogenesis involves a polyglutamine-independent step. J. Biol. Chem. 281, 16888–16896. http://dx.doi.org/10.1074/jbc.M601470200.

Goedert, M., Jakes, R., 1990. Expression of separate isoforms of human tau protein: correlation with the tau pattern in brain and effects on tubulin polymerization. EMBO J. 9, 4225–4230.

Goti, D., 2004. A mutant ataxin-3 putative-cleavage fragment in brains of Machado-Joseph disease patients and transgenic mice is cytotoxic above a critical concentration. J. Neurosci. 24, 10266–10279. http://dx.doi.org/10.1523/JNEUROSCI.2734-04.2004.

Hansen, S.K., Borland, H., Hasholt, L.F., Tümer, Z., Nielsen, J.E., Rasmussen, M.A., Nielsen, T.T., Stummann, T.C., Fog, K., Hyttel, P., 2016a. Generation of spinocerebellar ataxia type 3 patient-derived induced pluripotent stem cell line SCA3.A11. Stem Cell Res. 16, 553–556.

Hansen, S.K., Borland, H., Hasholt, L.F., Tümer, Z., Nielsen, J.E., Rasmussen, M.A., Nielsen, T.T., Stummann, T.C., Fog, K., Hyttel, P., 2016b. Generation of spinocerebellar ataxia type 3 patient-derived induced pluripotent stem cell line SCA3.B11. Stem Cell Res. 16, 589–592.

Heikkilä, T.J., Ylä-Outinen, L., Tanskanen, J.M.A., Lappalainen, R.S., Skottman, H., Suuronen, R., Mikkonen, J.E., Hyttinen, J.A.K., Narkilahti, S., 2009. Human embryonic stem cell-

derived neuronal cells form spontaneously active neuronal networks in vitro. Exp. Neurol. 218, 109–116. http://dx.doi.org/10.1016/j.expneurol.2009.04.011.
Hübener, J., Weber, J.J., Richter, C., Honold, L., Bellstedt, P., Weiss, A., Murad, F., Breuer, P., Wu, U., Paquet-durand, F., Takano, J., Saido, T.C., Riess, O., Nguyen, H.P., 2013. Calpain-mediated ataxin-3 cleavage in the molecular pathogenesis of spinocerebellar ataxia type 3 (SCA3). Hum. Mol. Genet. 22, 508–518. http://dx.doi.org/10.1093/hmg/dds449.
Kieling, C., Pr, P., Ml, S., Survival, J.L.B., 2007. Survival estimates for patients with Machado – Joseph disease (SCA3). Clin. Genet. 72, 543–545. http://dx.doi.org/10.1111/j.1399-0004.2007.00910.x.
Kirkeby, A., Grealish, S., Wolf, D.a., Nelander, J., Wood, J., Lundblad, M., Lindvall, O., Parmar, M., 2012. Generation of regionally specified neural progenitors and functional neurons from human embryonic stem cells under defined conditions. Cell Rep. 1, 703–714. http://dx.doi.org/10.1016/j.celrep.2012.04.009.
Kirwan, P., Turner-Bridger, B., Peter, M., Momoh, A., Arambepola, D., Robinson, H.P.C., Livesey, F.J., 2015. Development and function of human cerebral cortex neural networks from pluripotent stem cells in vitro. Development 142, 3178–3187. http://dx.doi.org/10.1242/dev.123851.
Koch, P., Breuer, P., Peitz, M., Jungverdorben, J., Kesavan, J., Poppe, D., Doerr, J., Ladewig, J., Mertens, J., Tüting, T., Hoffmann, P., Klockgether, T., Evert, B.O., Wüllner, U., Brüstle, O., 2011. Excitation-induced ataxin-3 aggregation in neurons from patients with Machado–Joseph disease. Nature 480, 0–5. http://dx.doi.org/10.1038/nature10671.
Matos, C.A., de Macedo-Ribeiro, S., Carvalho, A.L., 2011. Polyglutamine diseases: the special case of ataxin-3 and Machado–Joseph disease. Prog. Neurobiol. 95, 26–48. http://dx.doi.org/10.1016/j.pneurobio.2011.06.007.
Mori, F., Tanji, K., Odagiri, S., Toyoshima, Y., Yoshida, M., Kakita, A., Takahashi, H., Wakabayashi, K., 2012. Autophagy-related proteins (p62, NBR1 and LC3) in intranuclear inclusions in neurodegenerative diseases. Neurosci. Lett. 522, 134–138. http://dx.doi.org/10.1016/j.neulet.2012.06.026.
Myeku, N., Wang, H., Figueiredo-Pereira, M.E., 2012. CAMP stimulates the ubiquitin/proteasome pathway in rat spinal cord neurons. Neurosci. Lett. 527, 126–131. http://dx.doi.org/10.1016/j.neulet.2012.08.051.
Okita, K., Matsumura, Y., Sato, Y., Okada, A., Morizane, A., Okamoto, S., Hong, H., Nakagawa, M., Tanabe, K., Tezuka, K., Shibata, T., Kunisada, T., Takahashi, M., 2011. A more efficient method to generate integration-free human iPS cells. Nat. Methods 8, 409–412. http://dx.doi.org/10.1038/nmeth.1591.
Paulson, H.L., Das, S.S., Crino, P.B., Perez, M.K., Patel, S.C., Gotsdiner, D., Fischbeck, K.H., Pittman, R.N., 1997. Machado-Joseph disease gene product is a cytoplasmic protein widely expressed in brain. Ann. Neurol. 41, 453–462. http://dx.doi.org/10.1002/ana.410410408.
Pellistri, F., Bucciantini, M., Invernizzi, G., Gatta, E., Penco, A., Frana, A.M., Nosi, D., Relini, A., Regonesi, M.E., Gliozzi, A., Tortora, P., Robello, M., Stefani, M., 2013. Different ataxin-3 amyloid aggregates induce intracellular Ca^{2+} deregulation by different mechanisms in cerebellar granule cells. Biochim. Biophys. Acta, Mol. Cell Res. 1833, 3155–3165. http://dx.doi.org/10.1016/j.bbamcr.2013.08.019.
Philippidou, P., Dasen, J.S., 2013. Hox genes: choreographers in neural development, architects of circuit organization. Neuron 80, 12–34. http://dx.doi.org/10.1016/j.neuron.2013.09.020.
Rasmussen, M.A., Holst, B., Tümer, Z., Johnsen, M.G., Zhou, S., Stummann, T.C., Hyttel, P., Clausen, C., 2014. Transient p53 suppression increases reprogramming of human fibroblasts without affecting apoptosis and DNA damage. Stem Cell Rep. 3, 404–413. http://dx.doi.org/10.1016/j.stemcr.2014.07.006.
Robinson, H.P., Kawahara, M., Jimbo, Y., Torimitsu, K., Kuroda, Y., Kawana, a., 1993. Periodic synchronized bursting and intracellular calcium transients elicited by low magnesium in cultured cortical neurons. J. Neurophysiol. 70, 1606–1616.
Rüb, U., de Vos, R.A.I., Brunt, E.R., Sebestény, T., Schöls, L., Auburger, G., Bohl, J., Ghebremedhin, E., Gierga, K., Seidel, K., den Dunnen, W., Heinsen, H., Paulson, H., Deller, T., 2006. Spinocerebellar ataxia type 3 (SCA3): thalamic neurodegeneration occurs independently from thalamic ataxin-3 immunopositive neuronal intranuclear inclusions. Brain Pathol. 16, 218–227. http://dx.doi.org/10.1111/j.1750-3639.2006.00022.x.
Rüb, U., Brunt, E.R., Deller, T., 2008. New insights into the pathoanatomy of spinocerebellar ataxia type 3 (Machado-Joseph disease). Curr. Opin. Neurol. 21, 111–116. http://dx.doi.org/10.1097/WCO.0b013e3282f7673d.
Scherzed, W., Brunt, E.R., Heinsen, H., De Vos, R.a., Seidel, K., Bürk, K., Schöls, L., Auburger, G., Del Turco, D., Deller, T., Korf, H.W., Den Dunnen, W.F., Rüb, U., 2012. Pathoanatomy of cerebellar degeneration in spinocerebellar ataxia type 2 (SCA2) and type 3 (SCA3). Cerebellum 11, 749–760. http://dx.doi.org/10.1007/s12311-011-0340-8.
Silva-Fernandes, A., Costa, M.D.C., Duarte-Silva, S., Oliveira, P., Botelho, C.M., Martins, L., Mariz, J.A., Ferreira, T., Ribeiro, F., Correia-Neves, M., Costa, C., Maciel, P., 2010. Motor uncoordination and neuropathology in a transgenic mouse model of Machado-Joseph disease lacking intranuclear inclusions and ataxin-3 cleavage products. Neurobiol. Dis. 40, 163–176. http://dx.doi.org/10.1016/j.nbd.2010.05.021.
Sommer, C.A., Sommer, A.G., Longmire, T.A., Christodoulou, C., Thomas, D.D., Gostissa, M., Alt, F.W., Murphy, G.J., Kotton, D.N., Mostoslavsky, G., 2010. Excision of reprogramming transgenes improves the differentiation potential of iPS cells generated with a single excisable vector. Stem Cells 28, 64–74. http://dx.doi.org/10.1002/stem.255.
Sposito, T., Preza, E., Mahoney, C.J., Setó-Salvia, N., Ryan, N.S., Morris, H.R., Arber, C., Devine, M.J., Houlden, H., Warner, T.T., Bushell, T.J., Zagnoni, M., Kunath, T., Livesey, F.J., Fox, N.C., Rossor, M.N., Hardy, J., Wray, S., 2015. Developmental regulation of tau splicing is disrupted in stem cell-derived neurons from frontotemporal dementia patients with the 10 + 16 splice-site mutation in MAPT. Hum. Mol. Genet. 24, 5260–5269. http://dx.doi.org/10.1093/hmg/ddv246.
Sutor, B., Hagerty, T., 2005. Involvement of gap junctions in the development of the neocortex. Biochim. Biophys. Acta 1719, 59–68. http://dx.doi.org/10.1016/j.bbamem.2005.09.005.
Yamada, M., Tan, C.F., Inenaga, C., Tsuji, S., Takahashi, H., 2004. Sharing of polyglutamine localization by the neuronal nucleus and cytoplasm in CAG-repeat diseases. Neuropathol. Appl. Neurobiol. 30, 665–675. http://dx.doi.org/10.1111/j.1365-2990.2004.00583.x.
Yan, Y., Shin, S., Jha, B.s., Liu, Q., Sheng, J., Li, F., Zhan, M., Davis, J., Bharti, K., Zeng, X., Rao, M., Malik, N., Vemuri, M.C., 2013. Efficient and rapid derivation of primitive neural stem cells and generation of brain subtype neurons from human pluripotent stem cells. Stem Cells Transl. Med. 2, 862–870. http://dx.doi.org/10.5966/sctm.2013-0080.
Zhang, W., Liu, J., Sun, R., Zhao, L., Du, J., Ruan, C., Dai, K., 2011. Calpain activator dibucaine induces platelet apoptosis. Int. J. Mol. Sci. 12, 2125–2137. http://dx.doi.org/10.3390/ijms12042125.